

Studies of new Higgs boson interactions through nonresonant HH production in the $b\bar{b}\gamma\gamma$ final state in pp collisions at $\sqrt{s} = 13$ TeV with the ATLAS detector

Zihang Jia^{a,*} for the ATLAS collaboration

^aNanjing University,

No. 22 Hankou Rd., Gulou District, Nanjing, China

E-mail: zihang.jia@cern.ch

A search for nonresonant Higgs boson pair production in the $b\bar{b}\gamma\gamma$ final state is performed using 140 fb^{-1} of proton-proton collisions at a centre-of-mass energy of 13 TeV recorded by the ATLAS detector at the CERN Large Hadron Collider. This analysis supersedes and expands upon the previous nonresonant ATLAS results in this final state based on the same dataset. The analysis strategy is optimised to probe anomalous values not only of the Higgs (H) boson self-coupling modifier κ_λ but also of the quartic $HHVV$ ($V = W, Z$) coupling modifier κ_{2V} . No significant excess above the expected background from Standard Model processes is observed. An observed upper limit $\mu_{HH} < 4.0$ is set at 95% confidence level on the Higgs boson pair production cross-section normalised to its Standard Model prediction. The 95% confidence intervals for the coupling modifiers are $-1.4 < \kappa_\lambda < 6.9$ and $-0.5 < \kappa_{2V} < 2.7$, assuming all other Higgs boson couplings except the one under study are fixed to the Standard Model predictions. The results are then interpreted in the Standard Model effective field theory and Higgs effective field theory frameworks in terms of constraints on the couplings of anomalous Higgs boson (self-)interactions.

European Physical Society Conference for High Energy Physics - EPS-HEP 2023
21-25 August 2023
Universität Hamburg, Hamburg, Germany

*Speaker

1. Introduction

Since the discovery of a Higgs boson (H) in 2012, a priority of the ATLAS and CMS Collaborations has been to better understand its properties. All results obtained so far are consistent with the predictions of the Standard Model (SM). Remaining to be verified in the Higgs sector are those SM predictions for the coupling strengths of the interactions involving multiple Higgs bosons. A direct probe of the Higgs boson trilinear self-coupling ($\kappa_\lambda \equiv \lambda_{HHH}/\lambda_{HHH}^{\text{SM}}$) is possible via Higgs boson pair (HH) production. In the SM, gluon–gluon fusion (ggF) HH production proceeds through the destructive interference of two leading Feynman diagrams, as shown in Figure 1. The second-leading HH production process is vector boson fusion (VBF), as shown in Figure 2. The VBF production mode provides a unique sensitivity to the interaction between two Higgs bosons and two vector bosons ($\kappa_{2V} = g_{HHVV}/g_{HHVV}^{\text{SM}}$) and additional sensitivity to κ_λ . In the SM, the HH cross-sections are about three orders of magnitude smaller than those of single-Higgs boson production: $\sigma_{\text{ggF}}^{HH} = 31.05_{-7.20}^{+2.08}$ fb and $\sigma_{\text{VBF}}^{HH} = 1.73 \pm 0.04$ fb for $m_H = 125$ GeV.

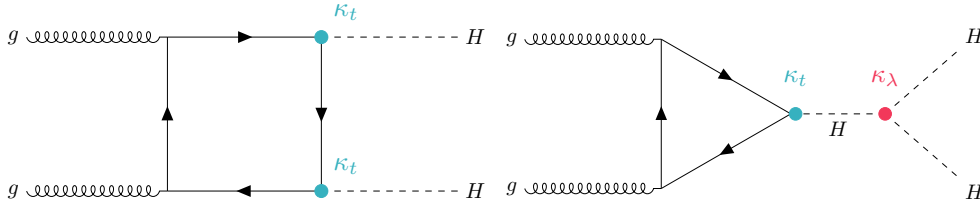


Figure 1: The Feynman diagrams for the ggF production mode.

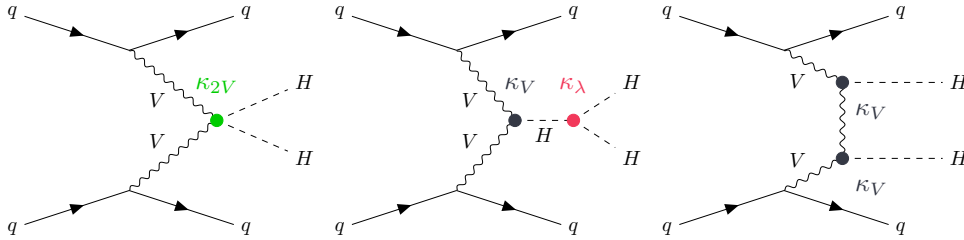


Figure 2: The Feynman diagrams for the VBF production mode.

The ATLAS experiment has released the results of searches based on the full Run 2 dataset in the three most sensitive channels, $b\bar{b}\gamma\gamma$ [1], $b\bar{b}\tau^+\tau^-$ [2], and $b\bar{b}b\bar{b}$ [3], and their combination [4]. The $b\bar{b}\gamma\gamma$ final state has an expected branching ratio (0.26%) that is significantly smaller than that of $b\bar{b}b\bar{b}$ (34%) and $b\bar{b}\tau^+\tau^-$ (7.3%). However, the larger expected signal-to-background (S/B) ratio and the larger acceptance in phase-space regions compensate for the lower expected event yield and lead to a sensitivity similar to that of the other two decay modes.

This article presents an updated search for nonresonant HH production in the $b\bar{b}\gamma\gamma$ final state using the full Run 2 ATLAS data. Compared to the previous publication, the classification of events in categories has been reoptimised, leading to a higher sensitivity to the κ_λ and κ_{2V} coupling modifiers. Another novelty is the interpretation of the results in two effective field theory (EFT) extensions of the Standard Model, the Higgs effective field theory (HEFT) [5, 6] and the Standard Model effective field theory (SMEFT) [7, 8].

2. Analysis strategy

2.1 Event selection and classification

To identify $H \rightarrow \gamma\gamma$ decays, events are collected with at least two photons satisfying the photon identification and isolation criteria. To target $H \rightarrow b\bar{b}$ decays, events are required to contain exactly two b -tagged jets passing the criteria of the ‘‘DL1r’’ b -tagging algorithm with an efficiency of 77% for b -jets in $t\bar{t}$ simulated events [9]. Events with more than five central jets, or with one or more isolated lepton (electron or muon) candidates are rejected in order to suppress $t\bar{t}H(\gamma\gamma)$ background.

After the preselections, events are classified in two regions based on the modified four-body invariant mass $m_{b\bar{b}\gamma\gamma}^* = m_{b\bar{b}\gamma\gamma} - m_{b\bar{b}} - m_{\gamma\gamma} + 250$ GeV with a boundary at 350 GeV. In each region, a dedicated boosted-decision-tree (BDT) discriminant is trained to distinguish HH signals from the background arising from $H \rightarrow \gamma\gamma$ decays in single-Higgs boson production events and from the continuum background from $t\bar{t}\gamma\gamma$ and $\gamma\gamma$ +jets events. The training is performed with the XGBoost program [10]. Compared to previous publication, additional kinematic features of the VBF HH signals featuring two additional highly energetic jets reconstructed in the forward regions are exploited. The VBF-jet candidates are determined by means of a dedicated BDT classifier, which is applied to all possible jet pair combinations in data and simulated events, and the jets belonging to the pair with the highest tagger score are considered as VBF-jet candidates.

After training, three categories in the high mass region and four categories in the low mass region are defined based on the BDT discriminants. Background-like events with lower BDT scores are discarded, as shown in Figure 3. The values of the BDT scores used to define the categories are chosen by maximising the combined number-counting significance of all categories using expected signal and background yields in the diphoton invariant mass range $120 \text{ GeV} < m_{\gamma\gamma} < 130 \text{ GeV}$.

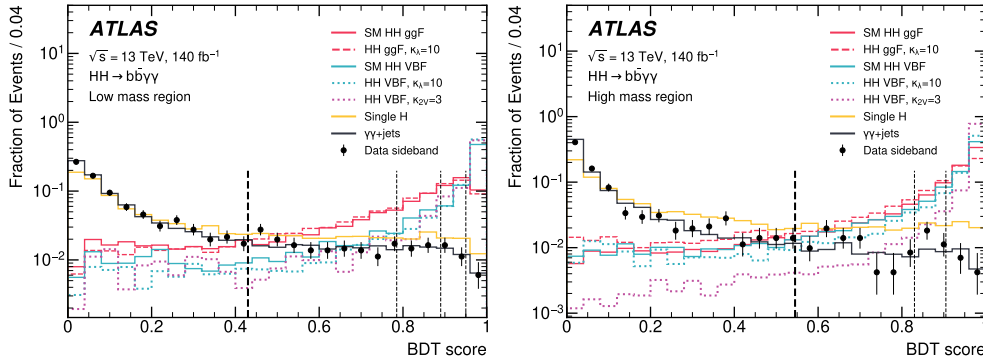


Figure 3: BDT score distributions for simulated HH signal and background events, as well as the data in the $m_{\gamma\gamma}$ sidebands. All distributions are normalised to unity.

2.2 Signal and background modelling

The signal, resonant and nonresonant background yields in each category are determined from unbinned maximum likelihood fits to the diphoton invariant mass distributions. The signal events and resonant single H background events are described by double-sided Crystal Ball functions [11, 12]. The continuum diphoton background are modelled with exponential functions, whose normalisation and shape parameters are obtained from the fit to the data.

3. Results

No evidence of signal is found. In the most sensitive categories of the analysis a small deficit of events in the signal region leads to a 95% CL upper limit on the HH production signal strength $\mu_{HH} < 4.0$ that is lower than the expected value of 5.0 (6.4) in the background-only $\mu_{HH} = 0$ (SM $\mu_{HH} = 1$) hypothesis. The corresponding observed (expected) one-dimensional intervals at 95% CL determined from one-dimensional scans of the profile likelihood function for the self-coupling modifier κ_λ and the quartic coupling modifier κ_{2V} are $-1.4 < \kappa_\lambda < 6.9$ ($-2.8 < \kappa_\lambda < 7.8$) and $-0.5 < \kappa_{2V} < 2.7$ ($-1.1 < \kappa_{2V} < 3.3$), respectively.

4. Effective field theory interpretation

Anomalous Higgs boson self-interactions or interactions with the other gauge fields and fermions can alter the Higgs boson pair production cross-section and kinematics, as well as the Higgs boson decay rates. The results of the previous section are thus interpreted in the context of two effective field theories to set constraints on the Wilson coefficients of the operators describing these anomalous interactions. In the HEFT interpretation, constraints on the coefficients c_{hhh} , c_{tthh} , and c_{gghh} that describe Higgs boson self-interactions as well as effective $t\bar{t}HH$ and $ggHH$ interactions are determined from one-dimensional scans of the profile likelihood function, as summarised in Table 1. In the SMEFT interpretation, constraints are set on two Wilson coefficients (c_H , $c_{H\Box}$) of the $(H^\dagger H)^3$ and $(H^\dagger H)\Box(H^\dagger H)$ operators of the ‘‘Warsaw’’ basis in the Standard Model effective field theory, as summarised in Table 2.

Wilson coefficient	95% CL Observed	95% CL Expected
c_{hhh}	[-1.7, 7.7]	[-3.4, 8.9]
c_{tthh}	[-0.28, 0.73]	[-0.48, 0.94]
c_{gghh}	[-0.42, 0.52]	[-0.59, 0.69]

Table 1: The observed and expected 95% CL constraints on the HEFT Wilson coefficients, obtained from one-dimensional scans of the profile log-likelihood under the assumption that all other Wilson coefficients are fixed to their SM values. The contribution from VBF HH production is subdominant to that from ggF and is neglected.

Wilson coefficient	95% CL Observed	95% CL Expected
c_H	[-14.4, 6.2]	[-16.8, 9.7]
$c_{H\Box}$	[-9.4, 10.2]	[-12.4, 13.7]

Table 2: The observed and expected 95% CL constraints on the SMEFT Wilson coefficients, obtained from one dimensional scans of the profile log-likelihood under the assumption that all other Wilson coefficients are fixed to their SM values. The contribution from VBF production is neglected.

References

- [1] ATLAS Collaboration, *Search for Higgs boson pair production in the two bottom quarks plus two photons final state in pp collisions at $\sqrt{s} = 13$ TeV with the ATLAS detector*, *Phys. Rev. D* **106** (2022) 052001 [2112.11876].
- [2] ATLAS Collaboration, *Search for resonant and non-resonant Higgs boson pair production in the $b\bar{b}\tau^+\tau^-$ decay channel using 13 TeV pp collision data from the ATLAS detector*, *JHEP* **07** (2023) 040 [2209.10910].
- [3] ATLAS Collaboration, *Search for nonresonant pair production of Higgs bosons in the $b\bar{b}b\bar{b}$ final state in pp collisions at $\sqrt{s} = 13$ TeV with the ATLAS detector*, *Phys. Rev. D* **108** (2023) 052003 [2301.03212].
- [4] ATLAS Collaboration, *Constraints on the Higgs boson self-coupling from single- and double-Higgs production with the ATLAS detector using pp collisions at $\sqrt{s} = 13$ TeV*, *Phys. Lett. B* **843** (2023) 137745 [2211.01216].
- [5] R. Alonso, M.B. Gavela, L. Merlo, S. Rigolin and J. Yepes, *The effective chiral Lagrangian for a light dynamical "Higgs particle"*, *Phys. Lett. B* **722** (2013) 330 [1212.3305].
- [6] G. Buchalla, O. Catà and C. Krause, *Complete electroweak chiral Lagrangian with a light Higgs at NLO*, *Nucl. Phys. B* **880** (2014) 552 [1307.5017].
- [7] W. Buchmüller and D. Wyler, *Effective lagrangian analysis of new interactions and flavour conservation*, *Nucl. Phys. B* **268** (1986) 621.
- [8] I. Brivio and M. Trott, *The standard model as an effective field theory*, *Phys. Rept.* **793** (2019) 1 [1706.08945].
- [9] ATLAS Collaboration, *ATLAS flavour-tagging algorithms for the LHC Run 2 pp collision dataset*, *Eur. Phys. J. C* **83** (2023) 681 [2211.16345].
- [10] T. Chen and C. Guestrin, *Xgboost: A scalable tree boosting system*, in *KDD 16*, pp. 785–794, (2016), DOI [1603.02754].
- [11] ATLAS Collaboration, *Measurement of Higgs boson production in the diphoton decay channel in pp collisions at center-of-mass energies of 7 and 8 TeV with the ATLAS detector*, *Phys. Rev. D* **90** (2014) 112015 [1408.7084].
- [12] M. Oreglia, *A Study of the Reactions $\psi' \rightarrow \gamma\gamma\psi$* , 1980.